

# System development and environmental performance analysis of a solar-driven supercritical water gasification pilot plant for hydrogen production using life cycle assessment approach

Jingwei Chen<sup>a,d</sup>, Wenwen Xu<sup>a</sup>, Hongyan Zuo<sup>c,\*</sup>, Xiaomin Wu<sup>b,\*</sup>, Jiaqiang E<sup>a,\*</sup>, Taosheng Wang<sup>c</sup>, Feng Zhang<sup>a</sup>, Na Lu<sup>d,e</sup>

<sup>a</sup> State Key Laboratory of Advanced Design and Manufacturing for Vehicle Body, Hunan University, Changsha 410082, China

<sup>b</sup> College of Liberal Arts and Sciences, National University of Defense Technology, Changsha 410073, China

<sup>c</sup> Business School, Hunan International Economics University, Changsha 410205, China

<sup>d</sup> Lyles School of Civil Engineering, Sustainable Materials and Renewable Technology (SMART) Lab, Purdue University, USA

<sup>e</sup> Materials Engineering and Birck Nanotechnology Center, Purdue University, USA

## ARTICLE INFO

### Keywords:

Biomass  
Solar energy  
Hydrogen production  
Supercritical water  
Pilot plant  
Life cycle assessment

## ABSTRACT

Supercritical water gasification (SCWG) of biomass is a promising technology for hydrogen production. A novel pilot plant of SCWG that uses solar energy (henceforth SCWG-Solar) was constructed in State Key Laboratory of Multiphase Flow in Power Engineering to take SCWG a significant step closer to industrialization. The total throughput of biomass and water was designed up to 1 t/h. Life cycle assessment (LCA) was conducted to evaluate the environmental performance of SCWG-Solar process and its main environmental burdens. LCA was conducted using the SimaPro V8.2.3 software, and the Ecoinvent 3.0 database within the program. A sensitivity analysis on crucial parameters was performed to determine the environmental performance enhancement of SCWG-Solar process. LCA results showed that the SCWG-Solar system operation contributes approximately 58% to the total environmental impact. The construction of a solar concentrator mostly contributes to the environmental emissions from the construction of the SCWG-Solar system. The environmental impact can be reduced by utilizing solar energy heated preheater and combining suitable post-treatment technologies of methane by-products with the SCWG-Solar system. The GWP decreases with the increase of feeding biomass slurry concentration and the GWP is close to a minimum when the biomass concentration reaches 30 wt%. GWP from the SCWG-Solar operation, which is 4.41 kg CO<sub>2</sub>-eq/kgH<sub>2</sub> for 1-MC process, is comparable to the solar based hydrogen production by two-step water splitting. Hence, the LCA in this study indicates that the SCWG-Solar is an environmentally friendly technology, although the system still has room for improvement.

## 1. Introduction

Fossil fuels have been used as the major energy source in recent decades [1,2]. However, the combustion of fossil fuels has caused serious pollution problems [3–6]. More attention has been paid to develop clean and new energy [7–9], e.g. hydrogen [10,11]. Hydrogen is a clean energy and is widely used in the energy, chemical, and transport sectors [12–14]. Currently, 96% of hydrogen is obtained from fossil resources, which cause direct CO<sub>2</sub>-emissions and other pollutions [15,16]. Traditional hydrogen production is energy-intensive and thus generally has large environmental impacts [17]. Hence, alternative hydrogen production routes with low environmental impacts, such as solar based hydrogen production technology, should be developed.

Various solar based hydrogen production routes were proposed, and solar thermochemical hydrogen production is considered to be industrialized in the near future. In the solar thermochemical process for hydrogen production, fossil fuels, water, and biomass are frequently used as hydrogen source, and solar energy is used as the high-temperature heat source [18,19]. A common solar thermochemical technology of hydrogen production includes water-splitting by thermochemical cycles, water thermolysis, and hybrid solar/fossil fuels processes [20,21]. Thereinto, a process that uses biomass as feedstock has many additional advantages. For example, all of the input energy, which are biomass and solar energy, are sustainable [22]. The process is CO<sub>2</sub> neutral in the entire life-time cycle because the plant photosynthesis for biomass growth consumes as much CO<sub>2</sub> as released during

\* Corresponding authors.

E-mail addresses: [zuohongyan18@126.com](mailto:zuohongyan18@126.com) (H. Zuo), [wuxiaomin@nudt.edu.cn](mailto:wuxiaomin@nudt.edu.cn) (X. Wu), [ejiaqiang@hnu.edu.cn](mailto:ejiaqiang@hnu.edu.cn) (J. E).

Nomenclature		FU	functional unit
GE	gasification efficiency, the total mass of product gas/the total mass of dry feedstock, %	SCW	supercritical water
HYP	hydrogen yield potential, the sum of measured hydrogen and the hydrogen which could theoretically be formed by completely shifting carbon monoxide and completely reforming hydrocarbon species, mol·kg <sup>-1</sup>	SCWG	supercritical water gasification
CE	carbon efficiency, the total carbon in the product gas/the total carbon in dry feedstock, %	SCWG-Solar	supercritical water gasification using concentrated solar energy
DNI	direct normal solar irradiation, W·m <sup>-2</sup>	LCA	life cycle assessment
		LCI	life cycle inventory
		LCIA	life cycle impact assessment
		SKLMF	State Key Laboratory of Multiphase Flow in Power Engineering
		CCS	carbon capture and storage

biomass utilization. On this basis, a research team in SKLMF proposed a novel solar based hydrogen production route, which is hydrogen production by SCWG of biomass that uses concentrated solar energy (henceforth to SCWG-Solar). SCWG has many advantages compared with other solar thermochemical technologies of hydrogen production due to several special properties of supercritical water [23,24]. For

example, biomass can be completely gasified in supercritical water at 600 °C. Wet biomass can be directly gasified through SCWG without drying [25,26], and thus SCWG process has high energy efficiency.

Modell [27,28] developed the first SCWG system in 1978. Subsequently, various science and technology issues about SCWG have been extensively investigated by many research institutes from the U.S.,

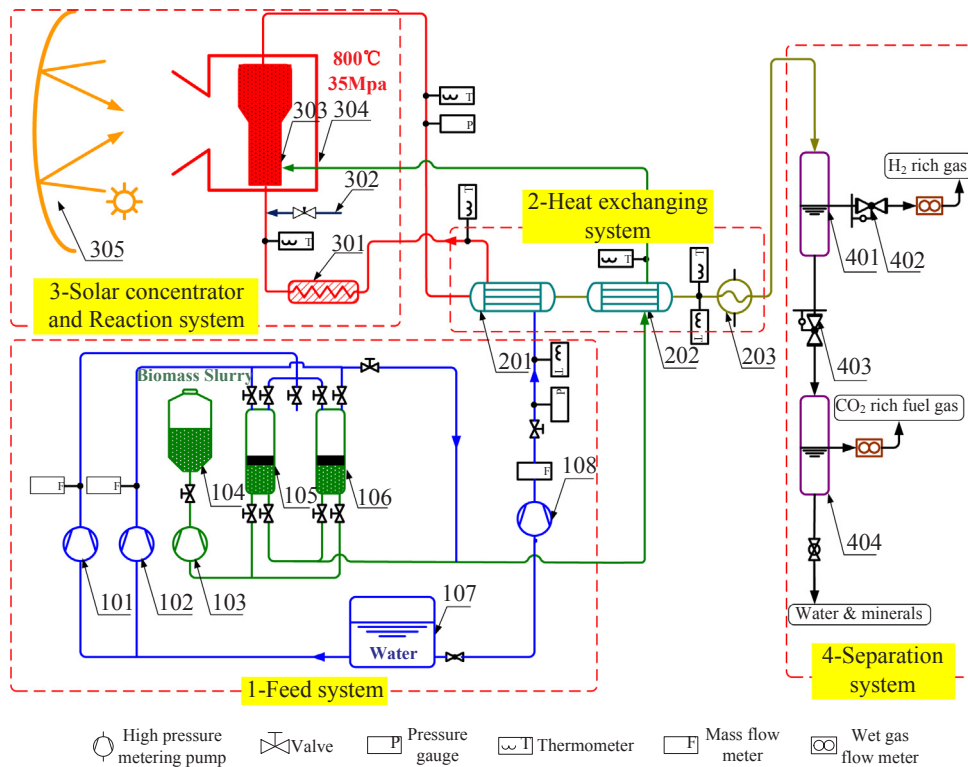


Fig. 1. Flow diagram of the pilot-scale SCWG-Solar system with the following design parameters:  $T_{max} = 800\text{ }^{\circ}\text{C}$ ,  $p_{max} = 35\text{ MPa}$ , throughput of biomass slurry = 1000 kg/h. 1-Biomass and Water Feed Sub-system; 2- Heat Exchanging System; 3- Solar Concentrator and Supercritical Water Reaction Sub-system; 4- Gas Separation and Collection Sub-system; 101,102-High-pressure Metering Pump; 103-Slurry Pump; 104-Feedstock stirred Tank; 105,106-Feeder; 107-Water Tank; 108-High-pressure Metering Pump; 201-Heat Exchanger; 202-Feedstock Heat Exchanger; 203-Cooler; 301-Preheater; 302-Reactor Chilling Unit; 303-Reactor Sub-system; 304-Solar Cavity Receiver; 305-Solar Concentrator; 401-High-pressure Separator; 402, 403-Back Pressure Regulator; 404-Low-pressure Separator.

1-Biomass and Water Feed Sub-system; 2- Heat Exchanging System; 3- Solar Concentrator and

Supercritical Water Reaction Sub-system; 4-Gas Separation and Collection Sub-system;

101,102-High-pressure Metering Pump; 103-Slurry Pump; 104-Feedstock stirred Tank; 105,106-Feeder;

107-Water Tank; 108-High-pressure Metering Pump; 201-Heat Exchanger; 202-Feedstock Heat Exchanger;

203-Cooler; 301-Preheater; 302-Reactor Chilling Unit; 303-Reactor Sub-system; 304-Solar Cavity

Receiver; 305-Solar Concentrator; 401-High-pressure Separator; 402, 403-Back Pressure Regulator;

404-Low-pressure Separator

Japan, Germany, and China [24,29]. In recent years, the SCWG system has been developed from laboratory to pilot scale with the progress of technology. Forschungszentrum Küste constructed the first pilot-scale system named “VERENA”, which has a design capacity of 100 L/h, to demonstrate supercritical gasification of wet residues from wine production [30]. Elliott et al. from the Pacific Northwest National Laboratory invented a transportable system designed at a scale of 1/2 t per day of wet feed to obtain engineering data for the scale-up of a system named TEES [31]. General Atomics constructed a SCWG and partial oxidation system, which was funded by U.S. Department of Energy, with a design handling capacity of biomass slurry of 200 kg/h [32]. In 2004, European Union subsidies and a grant awarded by the Japanese New Energy and Industrial Technology Development Organization enabled the construction of a well-equipped process development unit in Enschede, The Netherlands, with a maximum throughput capacity of 30 L/h [33]. In Japan, another pilot-scale SCWG system was constructed in Hiroshima University and has a 1 ton/day scale [34,35]. Recently, Yakaboylu et al. from Delft University of Technology reported the first results and experiences obtained from the TU Delft/Genos semi-pilot scale setup which has a capacity of 50 kg/h and incorporates a fluidized bed reactor [36]. In China, SKLMF developed many experimental systems for the hydrogen production of SCWG, such as the first system of supercritical water fluidized bed [37], various tubular reactor systems [10], and two laboratory-scale SCWG-Solar systems, namely, the dish and toroidal surface heliostat systems. Experimental tests and economic analysis on the SCWG-Solar system have validated the technical and economic feasibilities of its route [38,39]. Then, SKLMF developed the first pilot plant of SCWG-Solar to promote its commercialization process and reported the design parameters of the system in 2015 [40,41]. The authors of the present study have participated in the research on the pilot plant of SCWG-Solar with the funding from SKLMF. The development of a pilot-scale SCWG-Solar system, and the environmental impact assessment of SCWG-Solar have yet to be reported. Hence, the present work focuses on the aforementioned research contents.

For the assessment of environmental impacts, LCA is a tool that can promote industrial decision making toward sustainable resource management. LCA systematically investigates all the inputs and outputs of a system to evaluate the environmental impacts at all life cycle stages, which is from raw material extraction to final waste management [42]. In recent years, LCA has been widely used in hydrogen production technology to aid in the challenging decisions and determine the technology route that minimizes resources, emissions and costs [43,44]. Moreno and Dufour [45] assessed the environmental feasibility of hydrogen production through biomass gasification by investigating several feedstocks. Galera and Gutiérrez [46] evaluated the environmental performance of hydrogen and electricity production by supercritical water reforming (SCWR) of glycerol using the LCA approach. The results showed that the SCWR process is a suitable option for hydrogen production with the GWP of 3.77 kg CO<sub>2</sub>-eq per function unit. In

addition, the LCA of hydrogen production technologies that use several renewable energies, such as nuclear, wind, and solar energy, has been conducted to determine the major obstacles to overcome or the key issues to be solved to ensure the feasibility of these processes in recent years. Smitkova et al. [47] performed LCA for water-splitting thermochemical cycles (i.e., Westinghouse cycle and sulfur iodine cycles) that use heat energy from nuclear, solar and other sources. New hydrogen production processes, including water photo splitting, solar two-step thermochemical cycles, and solar electrolysis, have also been assessed using the LCA method. The results indicated that wind, hydro-power, and solar energy led to less environmental impact, compared with traditional hydrogen production technologies [42,48].

The main objective of this study is to investigate the environmental impact of solar based hydrogen production via a pilot plant of SCWG-Solar by performing a life cycle assessment (LCA). To the best of the authors' knowledge, study on performing the environmental performance of the SCWG-Solar is unavailable in the literature. Moreover, the engineering design and optimization of the pilot-scale SCWG system has not been investigated from the perspective of environmental impact. Thus, this work aims to address the aforementioned research gaps. The novel investigations of this work are expressed as follows:

(1) The environmental impact of the SCWG-Solar is evaluated by LCA to enhance the environmental performance of the SCWG-Solar system and determine the practical prospects and challenges for the SCWG-Solar technology. (2) The engineering optimization method of pilot-scale SCWG-Solar system is investigated by performing a sensitivity analysis on functional component and crucial parameters.

## 2. Methodology

### 2.1. Introduction of pilot plant

The schematic of the pilot-scale SCWG-Solar system is shown in Fig. 1. The pilot plant is designed using a modularization design method based on the different functions of the sub-subsystem. The pilot plant includes four sub-systems, namely, biomass and water feed, heat exchanging, solar concentrator and SCW reaction, and gas separation and collection sub-systems. The main components of the pilot-scale SCWG-Solar system comprises a solar concentrator, a solar receiver, SCW reactors, a biomass slurry feed system, heat exchangers, gas-liquid separators, and a product testing system.

#### 2.1.1. Solar concentrator

The photograph of the solar concentrator and its optical path are shown in Fig. 2. The solar concentrator named solar furnace was manufactured by the Chinese Academy of Sciences. It consists of three heliostats (two-axis tracking plane mirrors) that reflect solar rays onto a secondary parabolic concentrator to concentrate the sunlight to the aperture of the solar receiver. Ideally, each heliostat reflects the same number of solar rays to a part of the secondary concentrator that

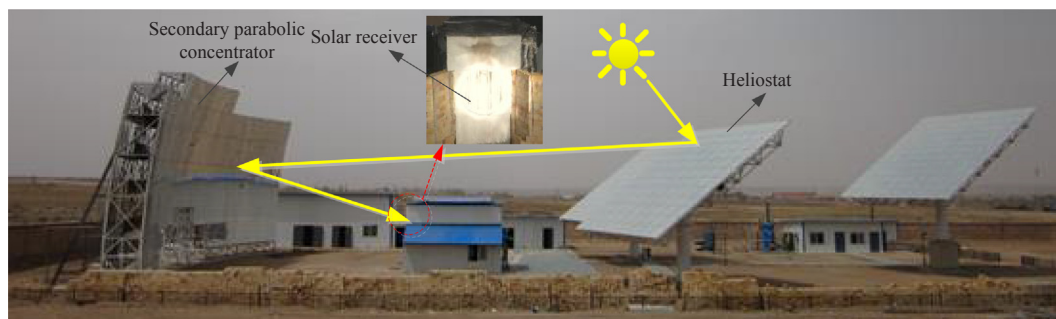


Fig. 2. Solar furnace concentrator, consisting of three heliostats that focus the sun's rays onto a secondary parabolic concentrator to concentrate the sunlight to the aperture of the solar receiver.

focuses the sunlight on the three specific surfaces of the receiver, and the supercritical water reactors are distributed on the inner surfaces of the solar receiver. In this way, heat flux is expected to be uniformly distributed in the reactors.

The area of the heliostat is 121 m<sup>2</sup>, and the area of the secondary parabolic concentrator is 300 m<sup>2</sup>. The diameter of the focal plane situated at the aperture of the solar receiver is 500 mm. The solar power delivered to the solar receiver is designed to be approximately 164 kW when the direct solar irradiation is 700 W/m<sup>2</sup>.

2.1.2. Operation procedures of the pilot plant

At the initial stage of the experiment, deionized water was directly pumped to the reactor by a high-pressure metering pump. The pressure of the system was regulated by the pressure regulator in the outlet of the system. Water was heated in the preheater and reactor. The biomass feedstock (wood sawdust) was fed to the reactor when the temperature and pressure of the system reached the setting value. The biomass feedstock (wood sawdust) was rapidly heated to a supercritical temperature by mixing with high-temperature preheated SCW. In the existing SCWG-Solar system, water was preheated by an electric heater. In the solar receiver, reactors were heated completely by concentrated solar irradiation and infrared radiation emitted by the hot inner walls of the cavity receiver. The designed temperature of solar receiver was 700 °C. The operation pressure of the SCWG system was 25 MPa. The drastic gasification reaction between the biomass and SCW occurred in the reactor. Subsequently, the effluent was transferred from the reactor to the heat exchangers. Heat of the effluent from the reactors was recovered in the heat exchangers using the preheated water. Thus, the temperature of the effluent decreased from 600 °C to approximately 250 °C and the preheated water was heated up from room temperature to 550 °C. Thereafter, the effluent flowed in the feedstock heat exchanger, wherein the effluent was cooled to < 200 °C and the biomass feedstock (wood sawdust) was heated from room temperature to approximately 200 °C. The effluent was then cooled to ambient temperature using a cooler, wherein the cooling water was heated from 25 °C to 50 °C and the maximum pressure of the cooling water stream

was 0.7 MPa. Subsequently, the cooling water was cooled to room temperature using a cooling tower and the cooling water was recycled. The pressure of the effluent was reduced to the pressure of the separators by using pressure regulators. In the high-pressure separator, H<sub>2</sub> and CH<sub>4</sub> were separated from the effluent, and CO<sub>2</sub> was dissolved in high-pressure water [49]. Finally, CO<sub>2</sub> was released in the low-pressure separator at ambient pressure.

SCWG is a complex process in which the biomass cracks into gaseous, liquid, and solid bioproducts, namely, syngas, bio-oil and char, respectively [50]. Most of the research on SCWG has used tubular reactors; however, the reactor plugging is a critical problem which is due to the formation of char and the accumulation of ash inside the reactor [51]. To solve the plugging problem, a unique design has been used in the SCWG-Solar system. The reactor used in this work was a supercritical water fluidized bed. The SCW went through the distributor at the bottom of the fluidized bed and biomass slurry entered the fluidized-bed from the entrance above the distributor. The instantaneous mixing of biomass and SCW could heat the biomass rapidly to improve H<sub>2</sub> yields and suppress char formation [10]. In addition, fluidized bed reactor provides a good heat and mass transfer that benefits the complete conversion of biomass and the suppression of the char production reaction [37,52]. Therefore, the amount of char produced by the SCWG-Solar system is small. In this study, a new configuration was designed at the bottom of the fluidized bed reactor in the SCWG-Solar system to collect the char and the deposited ash with inorganic salts which has an extremely low solubility in SCW and could be easily separated from the reaction system [50]. The collected char had a porous structure and contained a considerable amount of alkali and alkaline earth metals. These properties made char a favorable catalyst of SCWG-Solar system to enhance the H<sub>2</sub> yield and promote the phenol production in the aqueous phase [26,54]. After the separation of gaseous and solid products from the effluent, the liquid residual was collected after the back-pressure regulator and recycled to the SCWG-Solar system without separation of oil and water-soluble components. The main component of the liquid products was phenolic compounds and aldehydes. A system with the recycling liquid residual may increase the gasification

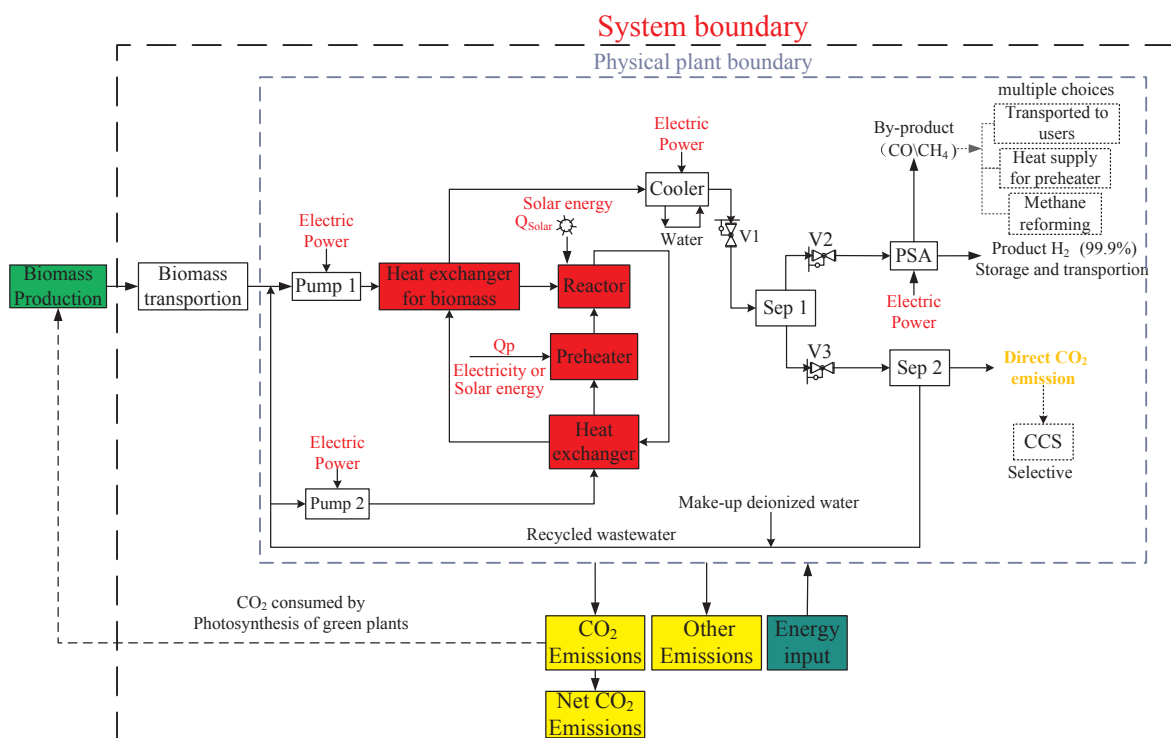


Fig. 3. System boundary for the LCA of the SCWG-Solar system.

efficiency and further decrease the TOC level [55]. Therefore, ash and wastewater could be collected and reused. The environmental impacts of ash and wastewater were neglected in this study.

## 2.2. Life cycle assessment

LCA is a systematic analytical method used in evaluating the potential environmental impact of a specific process in a cradle-to-grave manner to assess the environmental performance, identify the potential for environmental improvements, and compare alternative options. The LCA method has been formalized by the International Organization for Standardization. According to ISO-14044, the standard LCA process includes several steps [56], namely, goal and scope definition, life cycle inventory (LCI), life cycle impact assessment (LCIA), interpretation of the results, and overall assessment.

In this study, the LCA method was applied for the SCWG-Solar process. LCA evaluated the net emission of greenhouse gases and other major environmental consequences. It also identified the effects of key operation parameters and different equipment and stages of the SCWG-Solar in the life cycle time on the total environmental impacts. First, the system boundaries were defined. Second, the data for material and energy inputs and outputs of the process within the system boundaries were collected as a detailed LCI. Third, the environmental impacts associated with material and energy flows were evaluated based on the LCI. A sensitivity analysis was conducted to determine the effects of various factors, such as heating methods, carbon capture and storage (CCS), and the utilization method of by-products, on the environmental impacts in determining the optimization process. To provide the potential of SCWG-Solar process, its environmental impact was compared with that of other hydrogen production processes. Finally, conclusions and recommendations were provided.

### 2.2.1. Goal and scope definition

The system boundary “from the cradle to the grave,” which is the first step of LCA, is defined in Fig. 3. This step requires the specification of production processes and the input and output within the selected boundary. Inside the system boundary, the construction, operation and dismantling stages are considered. The entire lifetime of the system is set to 20 years. The construction stage involves assembly of the equipment, and production processes of raw materials. Dismantling stage involves the disassembly of the system, and recycling of some raw materials, such as steel and concrete. The operation stage involves the growth, collection and transportation of biomass; hydrogen production via SCWG coupled with solar heating; separation and purification of hydrogen-rich gas; and usage of final products.

The SCWG-Solar system includes high-pressure plunger pump 1 for biomass feeding, high-pressure plunger pump 2 for preheated water feeding, heat exchangers, coolers, preheater, SCW reactors, and gas-liquid separators. The wastewater could internally circulate during the gasification process, and the water consumed during the SCWG reaction will be further supplemented by deionized water. The amount of the make-up water would be described in Section 2.2.2. The char produced by the SCWG-Solar process was used as the catalyst of the SCW reactors, and the detail has been discussed in Section 2.1.2. Therefore, the environmental impact of the catalyst was not considered in this study. The high-pressure plunger pump consumed electricity. The SCW reactor was

heated by solar energy. The preheater could be heated by solar energy, electricity or byproduct combustion to identify the effects of heating methods on the environmental impacts, the details of which will be described in the subsequent section.

The system indirectly released carbon dioxide and several contaminants, such as acidic and nutrient substances, due to the raw materials and energy consumed by the construction and dismantling process, the consumption of fossil fuels during transportation, and the consumption of electricity, water, biomass during the operation stage of the pilot-scale system. In China, thermal power generation is the main source of grid power. Anthracite coal is the main coal type of thermal power plants which are located near to the SCWG-Solar system in this study. Therefore, in LCA software, the electricity consumed by the SCWG-Solar system was set to be obtained from the thermal power plant that uses anthracite coal as fuel. A functional unit (FU) is used as a reference unit in calculating the inputs and outputs. Thus, different systems could be compared on a common basis. In this study, the FU for the SCWG-Solar process was defined as the “production of 1 kg H<sub>2</sub>,” which is common for hydrogen production.

In this study, sensitivity analysis on the LCA of the SCWG-Solar system was conducted to determine the means of system optimization. First, the heating method of supercritical water reactors and preheater was used as an important parameter for sensitivity analysis. Thus, three heating methods were utilized for the SCWG-Solar process, and three types of corresponding process based on SCWG-Solar were defined, as follows:

- (1) The reactor and preheater were completely heated by solar energy, and the serial number of corresponding process was set to 1.
- (2) The reactors and preheater were heated by solar energy and electricity, respectively, and the serial number of the corresponding process was set to 2.
- (3) The reactors and preheater were heated by solar energy, and the by-product methane was combusted to supply heat to the system. The serial number of the corresponding process was set to 3.

Secondly, methane is a type of greenhouse gas; its greenhouse gas emission factor is approximately 25. Thus, methane should be appropriately handled to reduce the GWP of system. The three treatment methods of methane in this study are described as follows.

- (1) Methane was converted to hydrogen by steam reforming reaction, and the corresponding process was described based on the RF code.
- (2) Methane was recovered to supply combustion heat to the SCWG-Solar system, and the corresponding process was described based on the AT code.
- (3) Methane was collected and transported to the end-users for heat supply. The corresponding process was described based on the MC code.

In addition, CO<sub>2</sub> is a gaseous product of SCWG-Solar, which can be directly released to the atmosphere or captured and stored. The process of capture and storage of CO<sub>2</sub> produced by SCWG-Solar was represented by CCS. On the basis of the above assumptions, the investigated SCWG-Solar process can be divided into eight processes, namely, 1-MC, 1-RF, 1-RF-CCS, 2-MC, 2-RF, 2-RF-CCS, 3-AT, and 3-AT-CCS. Notably, the

**Table 1**  
Analysis data of wood sawdust being used [53].

Biomass type	Elemental Analysis (wt%)					Proximate analysis (wt%)				Calorific Value (MJ/kg)
	C	H	N	O <sup>a</sup>	S	M	A	V	FC	
Wood sawdust	46.76	5.27	0.11	38.47	0.03	8.00	1.36	77.12	13.52	16.70

<sup>a</sup> Difference.

basic procedure is the same for the eight processes except for the special assumptions and the current process of the existing SCWG-Solar system is 2-MC.

### 2.2.2. LCI analysis

In the LCA analysis, the total biomass and water treatment capacity of the SCWG-Solar system was set to 1.0 t/h. Moreover, the biomass was the raw biomass with 80% moisture content, which are located from areas 10 km away and was transported by road. Wood sawdust, which is represented by a general formula of  $\text{CH}_{1.35}\text{O}_{0.617}$  [49], was used as a typical gasification material in this work. The analysis data of the wood sawdust used are shown in Table 1 [57]. Notably, the SCWG of biomass has shown far-ranging of material applicability [10,58], and a large number of organic compounds, including wood sawdust, rice straw, wheat stalk, almond shell, corn stalk, corn cob, macroalgae, and coal, can be gasified in SCW using a pilot-scale SCWG-Solar system. Generally, the sulfur and nitrogen content of real biomass is small, approximately 0.03–0.25 wt% and 0.11–1.52 wt%, respectively [57]. N and S can be deposited as inorganic matter and be easily separated from the reaction system due to the low solubility of inorganic salts in supercritical water, element [40]. Therefore, N and S have minimal environmental impacts during the SCWG process and was thus neglected in this work. The raw biomass was processed using a grinder and a beater and was formulated into the biomass slurry. The biomass slurry was then delivered to the heat exchanger through a high-pressure

metering pump and heated to 250 °C and finally transported to the reactor. Water was delivered to a heat exchanger via a high-pressure plunger pump and was heated to 550 °C and then heated to 600 °C in the preheater. The main gaseous products of the SCWG-Solar were  $\text{H}_2$ ,  $\text{CH}_4$  and  $\text{CO}_2$ . The gasification data for LCA, which were calculated based on the chemical equilibrium, were cited from the work of Lu, et al. The chemical equilibrium model was based on minimization of Gibbs free energy [49]. Equations of State (Duan EOS) [59] put forward by Duan et al. was used to solve minimization of the Gibbs free energy. The mixture gas of  $\text{H}_2$  and  $\text{CH}_4$  underwent pressure swing adsorption (PSA) for  $\text{H}_2$  purification, and the final  $\text{H}_2$  purity reached 99.99%. High-purity hydrogen was collected online by using a high-pressure vessel and was transported to users 10 km away. Table 2 shows the detailed inventory data for the operation stage of the pilot-scale SCWG-Solar system. The mass and energy balance analysis about the pilot-scale SCWG-Solar system are described as follows:

The input material flows of the system included biomass slurry and water. The output material flows included liquid, gaseous and solid products. As described in Section 2.1.2, the effluent, including water and liquid products, was recycled to the system for the secondary gasification. The solid product and gaseous products were collected and used. As shown in Table 2, the moisture content of wet biomass was 80 wt% and the flow rate ratio between preheated water and feeding biomass slurry was 3. Therefore, the concentration of biomass slurry input into the reactor was 5 wt%. On the basis of chemical equilibrium,

**Table 2**  
Main inventory data for the operation stage of pilot-scale SCWG-Solar system.

Parameters	Value	Comments
Main operation parameters of the system		
Operation pressure of the reactor	25 MPa	
Operation temperature of the reactor	600 °C	
Temperature of biomass slurry at the reactor inlet	250 °C	
Temperature of the preheated water at the preheater outlet	600 °C	
Temperature of the preheated water at the preheater inlet	550 °C	Being equal to the water temperature at the outlet of heat exchanger
The flow rate ratio between preheated water and feeding biomass slurry	3	
Hydrogen purity	99.99%	PSA pressure is 30 bar
Transportation distance of the chemicals	10 km	Road transportation (18 t heavy-duty vehicle)
Heat resource of the reactor	Solar energy	
Functional unit	1 kg $\text{H}_2$	
Annual operating time	3000 h	
Operation years	20 years	
Mass balance		
Moisture content of wet biomass	80 wt%	Natural wet biomass
Chemical formula of biomass	$\text{CH}_{1.35}\text{O}_{0.617}$	Using the general chemical formula of biomass to define the elemental content of biomass.
Maximum flow rate of biomass slurry and water (mass input)	1000 $\text{kg}\cdot\text{h}^{-1}$	Material input of the system includes biomass and water. The flow rate of biomass slurry and water is 750 kg/h and 250 kg/h.
Gas yield of biomass gasification (mass output)	$\text{H}_2$ , 82.08 $\text{mol}\cdot\text{kg}^{-1}$ ; $\text{CH}_4$ , 1.67 $\text{mol}\cdot\text{kg}^{-1}$ ; $\text{CO}_2$ , 41.25 $\text{mol}\cdot\text{kg}^{-1}$ ;	Data were taken from chemical thermodynamic calculations under the conditions: 5 wt% concentration of biomass slurry input into the reactor (20 wt% feeding biomass slurry concentration), 600 °C, 25 MPa [49]
Wastewater at the outlet of the system (mass output)	900 $\text{kg}\cdot\text{h}^{-1}$	Including water and liquid products; internal recycling
Solid and liquid products (mass output)		Carbon conversion from raw materials to solid and liquid products was less than 1%; Solid products were reused as catalyst of the system.
Energy balance		
Solar energy per year supplied by solar concentrator (energy input)	806670.0 MJ	The local solar irradiation (from National Meteorological Information Center of China) is approximately $3448 \text{ MJ}\cdot\text{m}^{-2}$ per year; Solar concentration efficiency is 0.78
Energy input to the pumps (energy input)	0.014 $\text{kW}\cdot\text{h}\cdot\text{kg}^{-1}$	High-pressure biomass slurry and water pumps; Pump outlet pressure: 25 MPa; Work efficiency of the high-pressure pump is 50%.
Energy input to the cooler system (energy input)	0.6 $\text{kW}\cdot\text{h}$	Including energy input to the cooler pump and cooling tower
Energy required by the gasification of 1 kg biomass and water at the reactor (energy input)	817.2 $\text{kJ}\cdot\text{kg}^{-1}$	600 °C, 25 MPa, 20 wt% biomass slurry concentration; Thermal efficiency is 0.9
Energy required per kg of water at the preheater (energy input)	172.8 $\text{kJ}\cdot\text{kg}^{-1}$	550 °C – 600 °C, 25 MPa; Thermal efficiency is 0.9
Energy output	The calorific value of gaseous, liquid and solid products	The components of products were shown in the section of mass balance.

the gas yields of H<sub>2</sub>, CH<sub>4</sub> and CO<sub>2</sub> were 82.08, 1.67 and 41.25 mol/kg dry biomass, respectively, under the conditions of 600 °C and 25 MPa [49]. The theoretical carbon recovery ratio exceeded 99% from the biomass to the products. Notably, water is one of the reactants of the SCWG process. Therefore, a certain amount of water was consumed by the SCWG process. The mass of deionized water supplemented to the SCWG-Solar system per hour was approximately 50 kg when the total flow rate of biomass and water was 1000 kg/h.

The input energy of the SCWG-Solar system included the calorific value of biomass feed, energy required by the reactor and preheater and electricity consumed by the electric equipment, such as pump 1, pump 2 and cooler. The output energy of the SCWG-Solar system is the calorific value of gaseous, liquid and solid products. Solar energy has the natural property of intermittency. Direct solar irradiation changes continuously with the meteorological condition. Therefore, the throughput of SCWG-Solar system was continuously regulated on the basis of the direct solar irradiation. The pilot plant would shut down when solar power was unavailable because there is no auxiliary energy unit in the existing SCWG-Solar system. Therefore, according to the viewpoint of energy balance, the total hydrogen yield and biomass throughput of the system during its 20-year lifetime was calculated based on the total direct solar irradiation which could be supplied by solar concentrator. On the basis of the record of the direct solar irradiation from National Meteorological Information Center of China, the total direct solar irradiation of the location where SCWG-Solar system is located is approximately 3448 MJ/m<sup>2</sup> per year. The area and concentration efficiency of solar concentrator is 300 m<sup>2</sup> and 0.78, respectively. Therefore, the total solar irradiation for 20 years, which can be provided by the solar concentrator, is approximately 806670 MJ. In view of energy balance, the total solar irradiation was used to calculate the total output of hydrogen which could be produced by the SCWG-Solar system in its 20-year lifetime. The energy required by the SCWG of biomass included the heat of endothermic gasification reaction, energy required for the heating of water and biomass, and heat loss. The gasification reaction heat was calculated based on the difference of the lower heating value of reactants and products [60]. The lower heating value of the real biomass (wood sawdust) was 16.7 MJ/kg [57]. The heat required for the heating of biomass and water was calculated based on the sensible enthalpy difference. The detailed calculation method was adopted from the work of Lu et al. [49]. Heat loss was calculated based on the assumption that the thermal efficiency of the solar receiver was 90%. On the basis of above considerations, the reaction heat, heat required for heating of biomass and water and heat loss were 62, 144 and 21 kW, respectively, when the throughput of the SCWG-Solar system, temperature and pressure of the reactor was 1000 kg/h, 600 °C

and 25 MPa, respectively. Therefore, the energy required by the gasification of 1 kg biomass and water at the reactor was 817.2 kJ/kg biomass and water, as shown in Table 2. In addition, the energy required for the preheated water was 172.8 kJ per kg of water when the water was heated from 550 °C to 600 °C. The electricity consumed by the electric equipment was approximately 25 kW under the conditions shown in Table 2.

The PSA unit, which was used to separate H<sub>2</sub> and CH<sub>4</sub>, consumes 1.65 MJ of electricity for separation of 1 kg hydrogen [61]. CCS consumes approximately 0.66 MJ electricity for capture and storage of 1 kg CO<sub>2</sub> [56]. In consideration of a small amount of C<sub>2</sub>H<sub>4</sub> and C<sub>2</sub>H<sub>6</sub> in the actual gaseous product of SCWG [57], the process of byproduct methane steam reforming can refer to the natural gas steam reforming process. Natural gas steam reforming process consumes about 1.13 MJ electricity for 1 kg hydrogen production [62]. Notably, the solar energy supplied by the solar concentrator in the life-time of the eight processes was the same, which is determined by the design parameter of the solar concentrator and local solar irradiation. In view of the energy balance, the total amount of hydrogen produced by the SCWG-Solar system was calculated on the basis of the solar energy that could be supplied by the solar concentrator and the energy required by the SCWG of biomass (Table 2). The process, which included the auxiliary energy supply could produce more hydrogen than the process heated by solar energy entirely. Thus, 2-MC and 3-AT processes produced more hydrogen than 1-MC. The calculation results show that the total amounts of hydrogen produced by 1-MC, 2-MC and 3-AT in the 20-year lifetime were approximately 139864, 162045 and 150534 kg under the conditions shown in Table 2. In addition, 1-RF and 2-RF, which could convert byproduct methane to hydrogen, produce more hydrogen than the process without RF, and the total amounts of hydrogen produced by 1-RF, and 2-RF in the 20-year lifetime were approximately 151247 kg and 175233 kg, respectively.

In this study, data about the equipment, materials, scrap, and manufacturing processes of each device were from the SCWG-Solar pilot plant. The inventory data for the construction stage of the SCWG-Solar are shown in Table 3. For example, ultra-white glasses were used by the mirror of the solar concentrator, and 20# carbon steel was used by the truss of the solar concentrator. Q235 carbon, foundation concrete, and sand sub-crust were utilized in the foundation of equipment, such as the solar concentrator, pumps, heat exchangers, feeders, and water tanks. Nickel-based stainless steel was used as the main raw material for high-pressure pipes and equipment, such as the SCW reactors, preheater, heat exchangers, and high-pressure pipes. Aluminum silicate cotton was used for the insulation of high-temperature equipment. During the construction and assembly of the SCWG-Solar system,

**Table 3**  
LCI for the construction stage of SCWG-Solar.

Construction materials	Value	Unit	Transportation type and distance	Comments
Material type				
Ultra-white glass	3364	kg	Train or truck, 800 km	Solar mirrors
20# carbon steel	44,812	kg	Truck, 100 km	Section bar and square tube
Q235 carbon steel	7102	kg	Truck, 100 km	Embedded parts and rebar
2Cr13 stainless steel	7989	kg	Truck, 100 km	Steel bar
Nickel-based stainless steel	3226	kg	Train or truck, 620 km	Steel tube
Foundation concrete	375	m <sup>3</sup>	Truck, 100 km	C30 concrete
Sand subcrust	160	m <sup>3</sup>	Truck, 50 km	
Aluminum silicate insulation cotton	196	kg	Truck, 70 km	
Installation of equipment and pipes of SCWG				
Items	Value	Unit		
Welding consumables	44.2	kg		
Work consumption for weld	103.3	MJ		
Welding material type	ER316			
Installation of solar concentrator				
Welding consumables	192.0	kg		
Work consumption for weld	198.0	MJ		
Welding material type	J422			

electricity was consumed by the welding machine, drill, cutting machine, lathe, milling machine and several other material processing equipment. Particularly, plenty of welding materials were consumed by the welder.

The dismantling of the SCWG-Solar system includes plant disassembly and recycling or, when required, disposal of materials. The disposal scenario for the major materials is considered, as presented in Table 4 [63]. At the same time, the energy consumed during the dismantling of the system, such as the electricity consumed by the cutter, and the fuel used by the truck, is also considered.

### 2.2.3. Life cycle impact assessment

In this study, SimaPro V8.2.3, as well as the Ecoinvent 3.0 database within the program, was used in conducting LCA. In order to weight the potential impacts based on a common unit to assess the environmental performance of the research system, LCI data should be assigned to one or more categories and their corresponding indicators describing the causality chain [64]. On the basis of different characterization models, three LCIA methods were utilized to obtain different results in this work. These methods are CML-IA, ReCiPe Endpoint and Cumulative Energy Demand (CED). CML-IA (baseline V3.03/World 2000) was chosen as the midpoint assessment method (a problem-oriented approach) [65]. CML-IA provides detailed information on several environmental impact categories associated with hydrogen production systems and related processes, with relatively low level of uncertainty in quantitative methods. The midpoint impacts categories available in the CML-IA method, such as Global Warming Potential (GWP), Abiotic Depletion Potential (ADP), Acidification Potential (AP) and Eutrophication Potential (EP), Ozone Layer Depletion Potential (ODP) and Photochemical Oxidation Potential (POFP), were considered in the study. Notably, the midpoint method cannot provide a complete picture on the effect of impact pathway on the environment and three areas of protection, namely, Human Health, Ecosystem Quality, and Resource Scarcity. Thus, ReCiPe Endpoint (H) V1.12/World ReCiPe H/A was used as the endpoint assessment method to reflect the damage for the aforementioned areas of protection and normalize the damage categories to dimensionless points [66,67]. Finally, the CED method for open LCA was used to quantify the primary energy usage throughout the life cycle of the SCWG-Solar system. The CED method includes the direct and indirect uses of energy and ignores the waste used for energy purposes. In particular, fossil energy demand is responsible for the depletion of fossil fuels and global warming [68]. The LCA results and their interpretation will be discussed in the subsequent section.

## 3. Results and discussions

### 3.1. LCA results

#### 3.1.1. Sensitivity analysis of LCA

In this study, ADP, EP, ODP, GWP, POFP, and AP were selected as the representative midpoint categories based on the methodology of CML-IA baseline V3.03/World 2000. Fig. 4(a) and (b) show that a small gap exists between the different processes for ADP and ODP. ADP and ODP per FU of Process 2, which include the process of 2-MC, 2-RF and 2-RF-CCS, are smaller than other processes. The reason is that ADP and

ODP are mainly from the production of the construction materials which is the same for all processes, and the total amount of hydrogen produced by Process 2 is larger than that of other processes, as described in Section 2.2.2. Fig. 4(c) and (d) indicate that the total POFP and AP of 2-RF-CCS per FU are the highest, which are approximately 0.0076 kg C<sub>2</sub>H<sub>4</sub>-eq/kg H<sub>2</sub> and 0.19 kg SO<sub>2</sub>-eq/kg H<sub>2</sub>, respectively. POFP and AP are mainly from the operation stage of SCWG-Solar. Therefore, the total POFP and AP of Process 2, which consumes more electricity generated from the thermal power plant than that of others, including 2-MC, 2-RF, and 2-RF CCS, are larger than that of others. Fig. 4(e) shows that the variation of EP between different processes is small, and EP from the construction stage is larger than that of the operation stage. As shown in Fig. 4(f), the total GWP of 1-MC, 1-RF, 1-RF-CCS, 2-MC, 2-RF, 2-RF-CCS, 3-AT and 3-AT-CCS are 5.56, 5.21, -2.46, 10.95, 10.19, 2.52, 5.48 and -1.99 kg CO<sub>2</sub>-eq/kg H<sub>2</sub>. For the process without CCS equipment, GWP is mainly from the operation stage. GWPs from the operation stage of 2-MC and 2-RF are the largest, which are 9.95 and 9.27 kg CO<sub>2</sub>-eq/kg H<sub>2</sub>, respectively. Conversely, GWPs from the operation stage of 1-MC and 1-RF are the smallest, which are 4.41 and 4.15 kg CO<sub>2</sub>-eq/kg H<sub>2</sub>, respectively. Notably, GWPs from the operation stage of 1-RF-CCS and 3-AT-CCS are negative because the only carbon source in the SCWG-Solar process is biomass, and the carbon in the biomass is entirely neutral due to plant photosynthesis. Thus, in view of carbon footprint, the amount of CO<sub>2</sub> captured by CCS was set to a negative value, which is approximately -11.06 kg CO<sub>2</sub>-eq/kg H<sub>2</sub>. And it leads to a negative value of GWP for the process with CCS. Fig. 4(g) shows that the CEDs of Process 2 are higher than that of other processes, and the total CED of 2-RF-CCS is the highest. The required CED of the operation stage is larger than that of the construction stage. This result indicates that the operation of the SCWG-Solar system is a process that consumes more energy than the construction process. The reason for the results is that the electricity was required by the continuous operation of the equipment, such as high-pressure pumps, cooler, biomass treatment equipment and preheater of Process 2.

To compare the comprehensive environmental impacts of different processes, the normalization points based on ReCiPe Endpoint (H) V1.12 was used as the indicator. All of the midpoint categories were normalized to dimensionless points, which are valuable in identifying the comprehensive environmental impacts of a process. The higher dimensionless points mean greater environmental impacts. Fig. 5 shows that Human Health and Resources are the main environmental impacts for the SCWG-Solar system. The comprehensive environmental impacts of Process 2 (i.e., 2-MC, 2-RF, and 2-RF-CCS) are higher than that of other processes. The total normalization points of 1-MC, 1-RF, 2-RF and 3-AT are 0.00269, 0.00252, 0.00471 and 0.00265, respectively. The total normalization points of 2-MC are 1.9 times that of 1-MC, and the total normalization points of 1-RF-CCS, 2-RF-CCS and 3-AT-CCS are 1.43, 1.23 and 1.44 times that of 1-RF, 2-RF and 3-AT, respectively. These results reveal that Process 2 has the largest environmental emissions among the three types of SCWG-Solar processes. The combination of post-treatment technology of methane with SCWG-Solar can improve the environmental performance of the SCWG-Solar system, and the effect of methane reforming (RF) on the environmental performance is more obvious than that of supplement of heat by methane combustion (AT). The combination of methane steam reforming with

**Table 4**  
LCI of the dismantling stage of SCWG-Solar system.

Recycling fractions for the raw materials		Fractions (%)
Materials	Ecoinvent 3.0	
Concrete	Concrete, sole plate and foundation {CH}, concrete production, for civil engineering, with cement CEM I, Alloc Def, U	95
Unalloyed steel	Steel, unalloyed {RER}  steel production, converter, unalloyed   Alloc Def, U	90
Chromium steel	Steel, chromium steel 18/8 {RER}, steel production, converter, chromium steel 18/8, Alloc Def, U	90
Plant disassembly		Energy (MJ)
Work consumption for disassembly		121.9



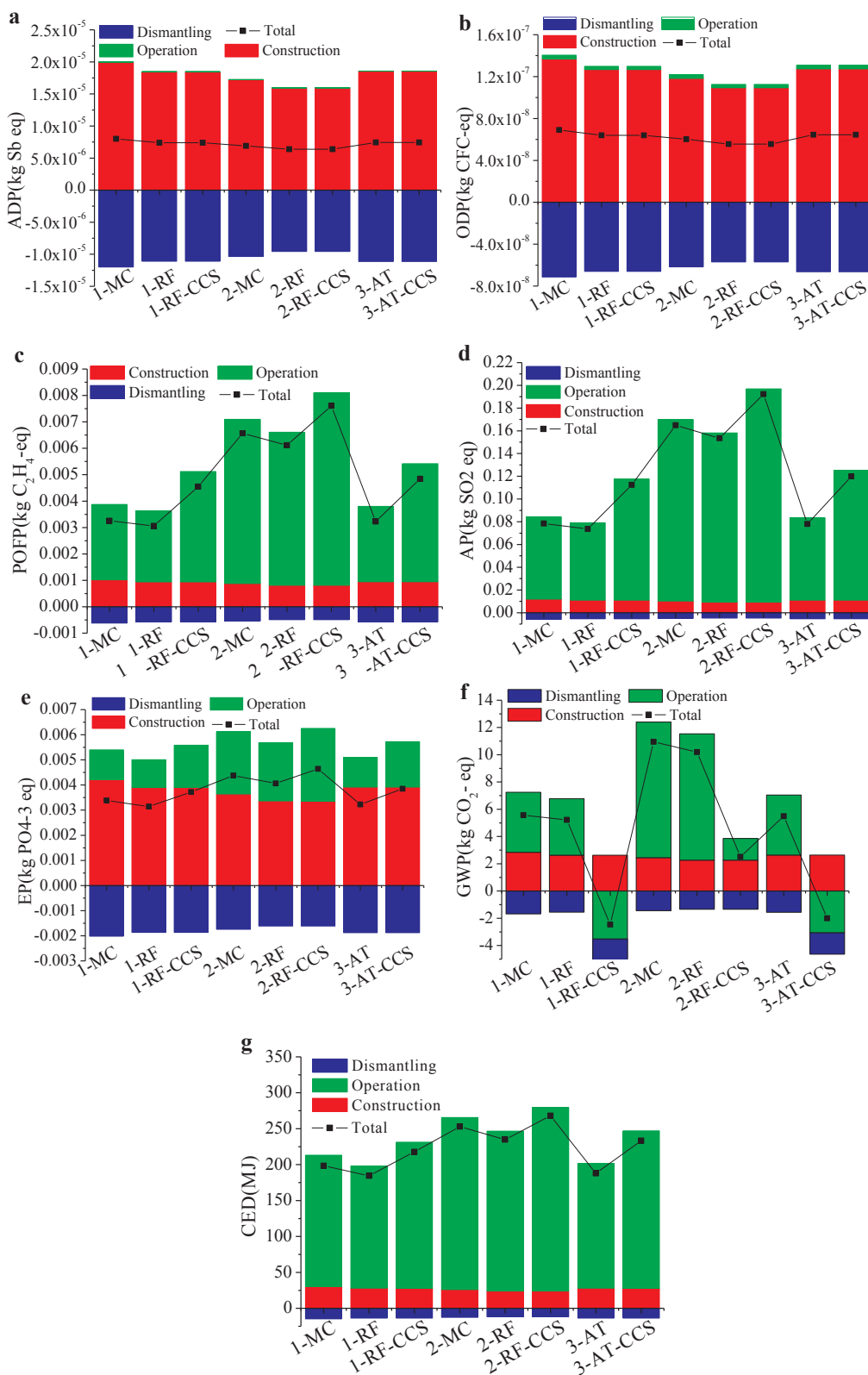


Fig. 4. Impact assessment results of the selected midpoint life cycle category.

SCWG-Solar can reduce the total environmental impact of SCWG-Solar by 6.3%. The use of solar energy instead of electricity as the energy source of the preheater is effective in reducing the environmental emissions of SCWG-Solar system. Moreover, CCS is valuable in reducing GWP but causes the increase of comprehensive environmental impacts

because it consumes electricity while collecting CO<sub>2</sub> [56]. Thus, the usage of CCS should be determined based on the goal of environment protection, which may focus on global warming or other types of environmental emission.

To determine the optimization method in detail of the

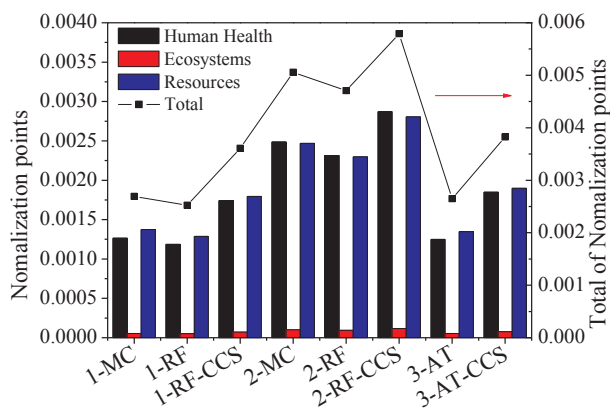


Fig. 5. Impact assessment results of the selected endpoint normalization points.

environmental performance of SCWG-Solar, the effect of different functional component on environmental impacts from the construction and operation stage will be discussed in Section 3.1.2.

3.1.2. Effect of process stage and functional component on environmental impacts

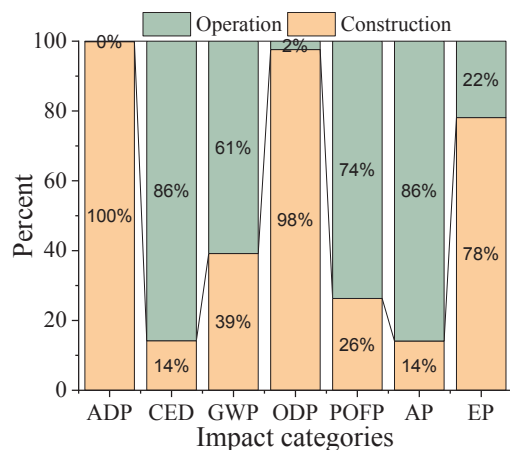
The LCA results of the selected midpoint and endpoint life cycle categories for process 1-MC are shown in Fig. 6. Fig. 6(a) indicates that the environmental emissions from the operation stage accounts for the most proportion of total emissions in terms of CED, GWP, POFP and AP, which are approximately 86%, 61%, 74%, and 86%, respectively. By contrast, several types of emission from the construction stage, such as ADP, ODP and EP, are more than that from the operation stage. Fig. 6(b) reveals that the comprehensive environmental impacts of the operation stage are greater than that of the construction stage, and the Resources impact of the SCWG-Solar is the largest among the three damage-oriented categories. For example, the operation stage accounts for 58% of the total environmental impacts, 68% of Human Health, 60% of Ecosystems, and 50% of Resources impacts. Fig. 6(b) also indicates that approximately 25% of the total environmental impacts of the entire process can be reduced by recycling several construction materials at the final dismantling stage of the SCWG-Solar system. Obviously, SCWG-Solar is still a new technology of solar based hydrogen and there is no experience about the disassembling and recycling of the SCWG-Solar. Thus, the amount of raw materials that can be recycled and the energy consumed by the disassembling process are assumed based on existing knowledges.

To determine the detailed source of environmental impacts, the percent of different environmental impacts from the different components of the SCWG-Solar system was calculated. The calculation results are shown in Fig. 7. As shown in Fig. 7(a), the construction of solar concentrator has the largest environmental impacts among all components. For example, the solar concentrator accounts for 78% of the total GWP from the construction of SCWG-Solar system. The environmental impacts of the construction stage are generally from two sources, which are the construction materials and the energy and materials consumed by processing equipment. The construction materials of solar concentrator mainly consist of ultra-white glass (3364 kg), 20# carbon steel of truss (44225 kg) and Q235 carbon steel of embedded parts (6095 kg). The construction materials of the solar concentrator are far more than that of SCWG equipment, including biomass feeder, heat exchanger, SCW reactor, cooler, and preheater. Thus, the optimization of the solar concentrator design, such as the optimization of the steel truss structure and the enhancement of the concentrating efficiency to reduce the reflective area, is the key strategy to reduce the environmental impacts from the construction stage. Fig. 7(b) shows the proportion of the normalization points of different parts during the operation stage, such as preheater, PSA, biomass treatment, cooler, pump

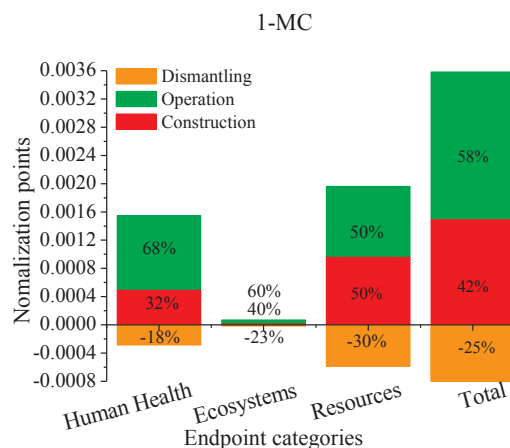
1, and pump 2. The results indicate that the operation of pump 2 has the largest environmental impact during the operation stage of 1-MC, which is about 43% and followed by cooler and pump 1. Differing from 1-MC, the operation of preheater accounts for the largest proportion of environmental impacts during the operation of 2-MC, which is about 59%. The difference between 1-MC and 2-MC is caused by the different heat source of preheater of 1-MC and 2-MC, which are solar energy and electricity, respectively. The use of the green electricity, such as solar and wind electricity [69], and the optimization of operation parameters to improve the energy efficiency can reduce the environmental impacts from the operation stage of the system.

3.1.3. Effect of feeding biomass slurry concentration on environmental impacts

GWP from the operation of 1-MC under different biomass concentration was analyzed in this study, as shown in Fig. 8. Notably, the biomass concentration mentioned in this study is the concentration of the biomass slurry fed by pump 1. In the reactor inlet, the biomass was mixed with the high-temperature preheated water. The ratio of mass flow rate of the preheated water to biomass slurry is 3. Thus, the real concentration of biomass that enters the supercritical water reactor is the quarter of the concentration of biomass slurry fed by pump 1. The gas yield was calculated based on the chemical equilibrium as the function of real biomass concentration inside the reactor [49], as shown in Fig. 9. It indicates that H<sub>2</sub> and CO<sub>2</sub> yields decrease gradually with

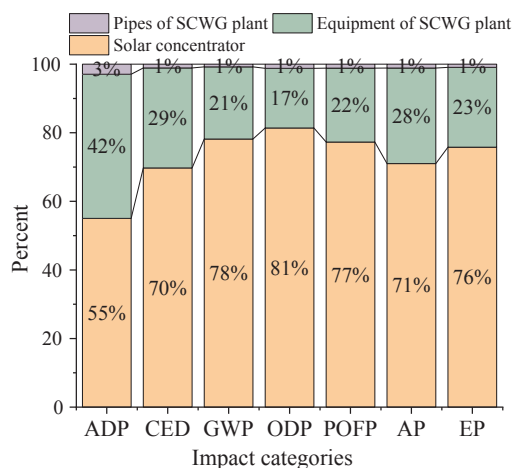


(a) Proportion of selected midpoint life cycle emissions from the operation and construction of process 1-MC

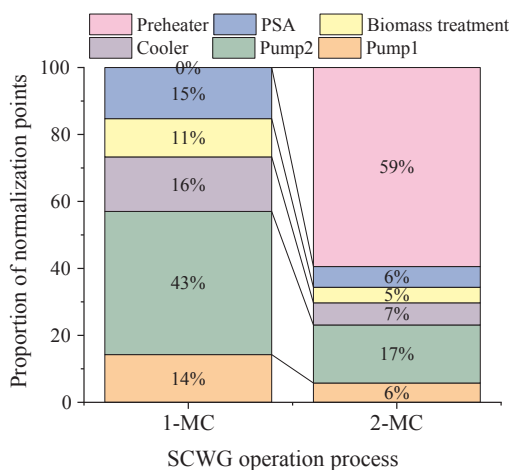


(b) Impact assessment results of endpoint normalization points for process 1-MC

Fig. 6. Impact assessment results of the selected midpoint and endpoint life cycle categories for process 1-MC.



(a) Proportion of selected midpoint life cycle emissions from different equipment of process 1-MC



(b) Proportion of endpoint normalization points of different equipment of processes 1-MC and 2-MC

Fig. 7. Proportion of the selected midpoint and endpoint life cycle categories of different equipment of processes 1-MC and 2-MC. (a) Proportion of selected midpoint life cycle emissions from different equipment of process 1-MC (b) Proportion of endpoint normalization points of different equipment of processes 1-MC and 2-MC.

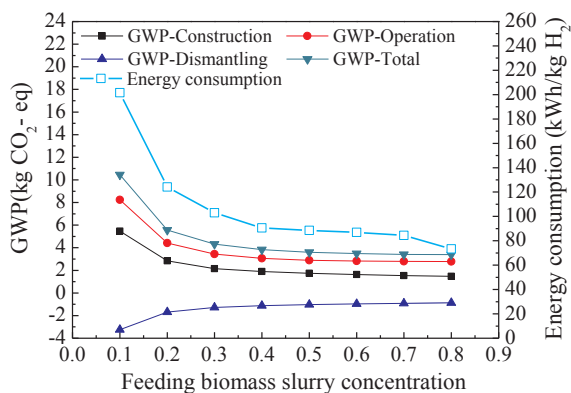


Fig. 8. GWP from the operation of 1-MC with different feeding biomass slurry concentrations.

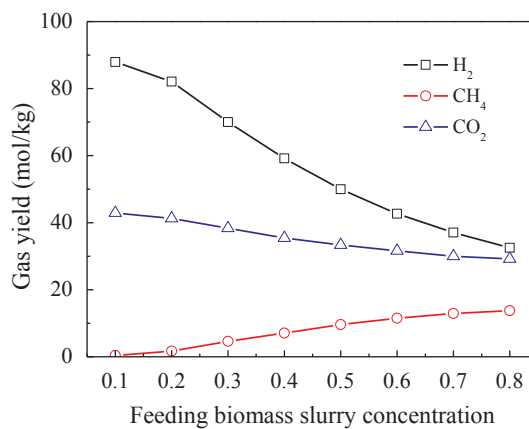


Fig. 9. Gas yields with different feeding biomass slurry concentrations.

increasing feedstock concentration, while the CH<sub>4</sub> yield increase. The variation trend of gas yields with the biomass concentration is similar with the previous works [26,55]. Fig. 8 reveals that the energy consumption per FU obviously decreases with the increase in biomass slurry concentration. At the same time, the GWP from the operation of 1-MC decreases from 8.23 kg CO<sub>2</sub>-eq/kg H<sub>2</sub> to 3.45 kg CO<sub>2</sub>-eq/kg H<sub>2</sub>, and the total GWP sharply decreases from 10.5 kg CO<sub>2</sub>-eq/kg H<sub>2</sub> to 4.32 kg CO<sub>2</sub>-eq/kg H<sub>2</sub> with the increase in biomass slurry concentration from 10 wt% to 30 wt%. Then, GWP changes little with the increase in concentration of biomass feedstock (wood sawdust). Thus, the biomass slurry concentration should be as high as 30 wt% in terms of environment protection. Moreover, it is well known that the dry-content of biomass feedstock should be high enough to ensure that the energy content of the feedstock is higher than the energy loss of the processing plant. For example, the required heat to reach 600 °C may exceed the energy content of biomass at a water content higher than 80% (g/g) [23]. However, the continuous feeding of biomass slurry with high content is a big problem. For example, the highest dry-matter content for which conventional high-pressure pumps can pump is usually up to 20 wt% [70,71]. In addition, the complete gasification of high-content biomass still faces great challenges. Although the biomass slurry feedstock concentration is difficult to increase due to the technical limitations, the biomass slurry feedstock concentration should exceed 20 wt%, even 30 wt% to meet the requirements of energy balance and environmentally friendly goal.

### 3.2. Comparison of environmental performance with other technologies

To compare the environmental performance of different hydrogen production technologies, GWP was selected as the typical indicator of environmental impacts. Table 5 shows the comparison results of GWP among different technologies, such as biomass conversion, natural gas and coal conversion, water electrolysis, representative solar based hydrogen production technology and SCWG-Solar. Notably, GWP of this study in Table 5 is obtained from the operation stage of the SCWG-Solar system. It can be seen that GWP of the traditional hydrogen production method by biomass gasification combined with steam reforming is the largest among the technologies of hydrogen production from biomass, which is approximately 18.97 kg CO<sub>2</sub>-eq/kg H<sub>2</sub> [72]. The GWP of biomass gasification coupled with combined cycle power generation-water electrolysis is approximately 4.11 kg CO<sub>2</sub>-eq/kg H<sub>2</sub>. These results show that the combined cycle power generation is a potential technology to reduce the environmental impact of the system, and the SCWG-Solar coupled with the combined cycle power generation technology will be investigated in future.

Generally, the GWP of hydrogen production from fossil fuels is extremely large. For example, the GWP of the steam reforming of natural gas, which is the main source of hydrogen in the energy market, is

**Table 5**  
Comparison of GWP with other studies.

Hydrogen production technology	GWP/kg CO <sub>2</sub> -eq·kg <sup>-1</sup> H <sub>2</sub>	Hydrogen production technology	GWP/kg CO <sub>2</sub> -eq·kg <sup>-1</sup> H <sub>2</sub>
Hydrogen production from biomass		Hydrogen production by nuclear based water-splitting	
Biomass gasification-catalytic steam reforming [72]	18.97	Nuclear based Cu–Cl water-splitting cycle [77]	15.8–0.56
Biomass gasification- Combined Cycle Power Generation –water electrolysis [72]	4.11	Nuclear based S–I water-splitting cycle [78,79]	2.5–0.41
Steam reforming of biomass [80]	6.26	Nuclear based ISPRA Mark 9 water-splitting cycle [81]	2.5
Hydrogen production from fossil fuels		Solar based hydrogen production [42]	
Steam reforming of natural gas [17]	10.67	Water photosplitting with CdZnS	0.55
Steam reforming of natural gas with CCS [82]	3.51	Water photosplitting with CdS-ZnS-ZnO	0.62
Underground coal gasification [73]	18	Two-step thermochemical cycles with ZnO	4.74
Underground coal gasification with CCS [69]	0.91	Two-step thermochemical cycles with NiFe <sub>2</sub> O <sub>4</sub>	4.67
Water electrolysis		This work	
Photovoltaic generation- water electrolysis [17]	5.85	1-MC	4.41
Wind power generation- water electrolysis [17]	1.35	1-RF	4.15
Nuclear energy-high temperature water electrolysis [74]	1.98	1-RF-CCS	–3.53
Electricity grid- water electrolysis [42]	25.93		

approximately 10.67 kg CO<sub>2</sub> eq/kg H<sub>2</sub> [17]. And GWP of underground coal gasification is approximately 18 kg CO<sub>2</sub>-eq/kg H<sub>2</sub>, which decreases to 0.91 kg CO<sub>2</sub>-eq/kg H<sub>2</sub> when CCS is used [73]. For hydrogen production by water electrolysis, the traditional water electrolysis by grid electricity is large, which is about 25.93 kgCO<sub>2</sub>-eq/kg H<sub>2</sub> [38]. When the green electricity was applied to the water electrolysis instead of grid electricity, the GWP of water electrolysis sharply decreases (e.g., 1.35 kg CO<sub>2</sub>-eq/kg H<sub>2</sub> for wind electricity-water electrolysis [17], and 1.98 kg CO<sub>2</sub>-eq/kg H<sub>2</sub> for nuclear energy-high temperature water electrolysis [74]).

Thermochemical water splitting has recently been considered as a promising hydrogen production route [75]. The following cycles have been identified as of possible commercial significance: sulphur–iodine (S–I), copper–chlorine (Cu–Cl), ZnO/Zn and Fe<sub>3</sub>O<sub>4</sub>/FeO redox reactions [76]. Thermochemical water splitting based on renewable and nuclear resources has been considered as a promising alternative for H<sub>2</sub> production [77]. If electrical energy output of the nuclear plant is used for all processes in nuclear-based hydrogen production, then the GWP of nuclear based Cu–Cl water splitting cycle decreases from an initial value of 15.8 kg to 0.56 kg CO<sub>2</sub>-eq/kg H<sub>2</sub> [77] and the GWP of the nuclear based S–I water-splitting cycle decreases from 2.5 kg to 0.41 kg CO<sub>2</sub>-eq/kg H<sub>2</sub> [78,79]. The GWPs of solar based two-step thermochemical water splitting by ZnO and NiFe<sub>2</sub>O<sub>4</sub> are approximately 4.74 kg CO<sub>2</sub>-eq/kg H<sub>2</sub> and 4.67 kg CO<sub>2</sub>-eq/kg H<sub>2</sub>, respectively [42], respectively. In addition, the GWP of photocatalytic water splitting is extremely small. However, thus far, the efficiency of hydrogen production of photocatalytic water splitting remains low. In this work, the GWP of 1-MC is 4.41 kg CO<sub>2</sub>-eq/kg H<sub>2</sub> and reaches 4.15 kg CO<sub>2</sub>-eq/kg H<sub>2</sub> when steam reforming is combined with 1-MC. Furthermore, GWP becomes negative when 1-RF is coupled with CCS, which is approximately –3.35 kg CO<sub>2</sub>-eq/kg H<sub>2</sub>. Thus, GWPs of 1-MC and 1-RF are comparative with biomass gasification-combined cycle power generation-water electrolysis and solar thermochemical hydrogen production by two-step water splitting. Although the GWP of 1-MC is more than that of thermochemical water-splitting cycle which is entirely driven by nuclear energy, the GWP of the SCWG-Solar can be expected to be close to that of the nuclear based water-splitting cycle if green electricity is used by the SCWG-Solar system instead of thermal electricity. The preceding comparison results reveal that SCWG-Solar is an environmentally friendly and sustainable technology of hydrogen production, which has a great prospect for large-scale application. Meanwhile, a large environmental potential exists in the optimization of the technical parameters and the system design for the existing pilot plant of SCWG-Solar system.

### 3.3. Future work in terms of challenges and chances

The SCWG-Solar system is extended from laboratory to pilot scale. However, several challenges must still be overcome, as detailed as follows.

(1) The development of the pilot-scale SCWG-Solar system is the first step. However, detailed experimental results with the pilot plant, including the effects of operation parameters on biomass gasification, reaction kinetics of SCWG in the pilot-scale system, and thermal characteristic of solar receiver applied for SCWG-Solar, are not reported.

(2) The pilot system can be optimized based on LCA. For example, CCS can be used to reduce the greenhouse gas emissions of the system. The appropriate use of by-product methane can be beneficial to the environmental performance of SCWG-Solar, such as steam reforming of methane or methane as the supplementary heat source of the system. Moreover, the combination of cycle power generation with SCWG is a good method to enhance the energy efficiency and environmental performance of the SCWG-Solar. The aforementioned inference should be confirmed based on the research of LCA and energy analysis in the future.

(3) Operation parameters, such as the biomass concentration of feeding biomass slurry should be optimized for SCWG-Solar. In this study, the results show that 30 wt% is the reasonable biomass concentration. However, the feeding and complete gasification of biomass slurry with high content experience considerable challenges, which may determine the future of SCWG-Solar technology.

## 4. Conclusion

A novel pilot plant of SCWG-Solar system with 1 t/h throughput of biomass and water was successfully constructed and operated in SKLMF. On the basis of the pilot-scale SCWG-Solar system, LCA was conducted using SimaPro V8.2.3 software to evaluate the environmental performance and identify the environmental burdens of SCWG-Solar. Sensitivity analysis of LCA was conducted, and the effects of functional component and biomass slurry concentration on the environmental impact were analyzed to obtain the optimization method of the system. The results showed that the environmental impact of the system operation contributes 58% of the total environmental impact for process 1-MC. The construction of the solar concentrator accounts for the most of the environmental emissions during the construction of the system (i.e., 78% of the total GWP). The environmental impact increases by 90% when the preheater is heated by thermal electricity instead of solar energy. Moreover, the combination of methane steam reforming with SCWG-Solar could reduce the total environmental impact by 6.3%. CCS is valuable in reducing the GWP but increased the total environmental impact. The GWP decreases with the increase of

feeding biomass slurry concentration and a 30 wt% concentration is reasonable to bring GWP close to a minimum. The GWP for the operation of 1-MC process, which is 4.41 kg CO<sub>2</sub>/kg H<sub>2</sub>, is comparative with the solar thermochemical hydrogen production by two-step water splitting. The LCA results confirm that SCWG-Solar is an environmentally friendly solar based hydrogen technology. Nonetheless, its environmental performance could be further optimized through the process optimization suggested in this study.

### Conflict of interests

The authors declare that they have no conflict of interests regarding the publication of this paper.

### Acknowledgements

This work was financially supported by the National Natural Science Foundation of China (Contract NO. 51508176 and 71573082), Fundamental Research Funds for the Central Universities, Key Projects of Hunan Province Science and Technology Plan (NO. 2018SK2019); Hunan province innovation platform open fund (NO. 14K055), Fund project [2017JJ2134] supported by Natural Science Foundation Project of Hunan Province and Open Foundation of State Key Laboratory of Multiphase Flow in Power Engineering of China.

### References

- Nicoletti G, Arcuri N, Nicoletti G, Bruno R. A technical and environmental comparison between hydrogen and some fossil fuels. *Energy Convers Manage* 2015;89:205–13.
- Lin B, Ouyang X. A revisit of fossil-fuel subsidies in China: challenges and opportunities for energy price reform. *Energy Convers Manage* 2014;82:124–34.
- E J, Zhao X, Xie L, Zhang B, Chen J, Zuo Q, et al. Performance enhancement of microwave assisted regeneration in a wall-flow diesel particulate filter based on field synergy theory. *Energy*. 2019;169:719–29.
- Zhang B, E J, Gong J, Yuan W, Zhao X, Hu W. Influence of structural and operating factors on performance degradation of the diesel particulate filter based on composite regeneration. *Appl Therm Eng* 2017;121:838–52.
- Deng Y, Zheng W, E J, Zhang B, Zhao X, Zuo Q, Zhang Z, Han D. Influence of geometric characteristics of a diesel particulate filter on its behavior in equilibrium state. *Appl Therm Eng* 2017;123:61–73.
- Deng Y, Cui J, E J, Zhang B, Zhao X, Zhang Z, Han D. Investigations on the temperature distribution of the diesel particulate filter in the thermal regeneration process and its field synergy analysis. *Appl Therm Eng* 2017;123:92–102.
- Zhang Z, E J, Chen J, Zhu H, Zhao X, Han D, Zuo W, Peng Q, Gong J, Yin Z. Effects of different water additive rate on spray, combustion and emission characteristics of a medium speed diesel engine fueled with biodiesel fuel. *Fuel* 2019;239:245–62.
- E J, Zhang Z, Chen J, Pham MH, Zhao X, Peng Q, Zuo W, Yin Z. Performance and emission evaluation of a marine diesel engine fueled by water biodiesel-diesel emulsion blends with a fuel additive of a cerium oxide nanoparticle. *Energy Convers Manage* 2018;169:194–205.
- Chen J, Fan Y, E J, Cao W, Zhang F, Gong J, Liu G, Xu W. Effects analysis on the reaction kinetic characteristics of the food waste gasification by supercritical water. *Fuel* 2019;241:94–104.
- Guo LJ, Lu YJ, Zhang XM, Ji CM, Guan Y, Pei AX. Hydrogen production by biomass gasification in supercritical water: a systematic experimental and analytical study. *Catal Today* 2007;129:275–86.
- Li Y, Liu G, Rao Z, Liao S. Field synergy principle analysis for reducing natural convection heat loss of a solar cavity receiver. *Renewable Energy* 2015;75:257–65.
- E J, Peng Q, Liu X, Zuo W, Zhao X, Liu H. Numerical investigation on hydrogen/air non-premixed combustion in a three-dimensional micro combustor. *Energy Conv Manag*. 2016;124:427–38.
- Zuo W, E J, Lin RM, Jin Y, Han DD. Numerical investigations on different configurations of a four-channel meso-scale planar combustor fueled by hydrogen/air mixture. *Energy Conv Manag*. 2018;160:1–13.
- Peng Q, E J, Chen J, Zuo W, Zhao X, Zhang Z. Investigation on the effects of wall thickness and porous media on the thermal performance of a non-premixed hydrogen fueled cylindrical micro combustor. *Energy Conv Manag*. 2018;155:276–86.
- Simbollotti GIEA. Energy technology essentials-hydrogen production and distribution. *Int. Energy*. 2017:544.
- Zhou D, Tay KL, Tu Y, Li J, Yang W, Zhao D. A numerical investigation on the injection timing of boot injection rate-shapes in a kerosene-diesel engine with a clustered dynamic adaptive chemistry method. *Appl Energy* 2018;220:117–26.
- Koroneos C, Dompros A, Roumbas G, Moussiopoulos N. Life cycle assessment of hydrogen fuel production processes. *Int J Hydrogen Energy* 2004;29:1443–50.
- Al-Nimr MA, Al-Darawsheh IA, Al-Khalayleh LA. A novel hybrid cavity solar thermal collector. *Renewable Energy* 2018;115:299–307.
- Liu GL, E J, Liu T, Zuo W, Zhang QL. Effects of different poses and wind speeds on flow field of dish solar concentrator based on virtual wind tunnel experiment with constant wind. *J Cent South Univ* 2018;25:1948–57.
- Fletcher EA. Solarthermal processing: a review. *J Sol Energ-T Asme*. 2001;123:63–74.
- Aldo S. Solar thermochemical production of hydrogen—a review. *Sol Energy* 2005;78:603–15.
- Li Y, Liu G, Liu X, Liao S. Thermodynamic multi-objective optimization of a solar-dish Brayton system based on maximum power output, thermal efficiency and ecological performance. *Renewable Energy* 2016;95:465–73.
- Kruse A. Hydrothermal biomass gasification. *J Supercritical Fluids* 2009;47:391–9.
- van Rossum G, Potic B, Kersten SRA, van Swaaij WPM. Catalytic gasification of dry and wet biomass. *Catal Today* 2009;145:10–8.
- Norouzi O, Safari F, Jafarian S, Tavasoli A, Karimi A. Hydrothermal gasification performance of *Enteromorpha intestinalis* as an algal biomass for hydrogen-rich gas production using Ru promoted Fe-Ni/γ-Al<sub>2</sub>O<sub>3</sub> nanocatalysts. *Energy Convers Manage* 2017;141:63–71.
- Safari F, Javani N, Yumurtaci Z. Hydrogen production via supercritical water gasification of almond shell over algal and agricultural hydrochars as catalysts. *Int J Hydrogen Energy* 2018;43:1071–80.
- Modell M. Processing methods for the oxidation of organics in supercritical water. *US Patent* 1982;4(338):199.
- Modell M, Reid R, Amin S. Gasification process. *US Patent* 1978;4(113):446.
- Kruse A. Supercritical water gasification. *Biofuels, Bioprod Biorefin* 2008;2:415–37.
- Boukis N, Galla U, Müller H, Dinjus E. Biomass gasification in supercritical water. Experimental progress achieved with the VERENA pilot plant. In: 15th European Biomass Conference & Exhibition. Berlin 2007. p. 1013–6.
- Elliott DC, Neuenschwander GG, Phelps MR, Hart TR, Zacher AH, Silva LJ. Chemical Processing in High-Pressure Aqueous Environments. 6. Demonstration of Catalytic Gasification for Chemical Manufacturing Wastewater Cleanup in Industrial Plants. *Ind Eng Chem Res* 1999;38:879–83.
- Hong GT, Spritzer MH. Supercritical water partial oxidation. Proceedings of the 2002 U. S. DOE Hydrogen Program Review. p. NREL/CP-610-32405.
- Potic B, Kersten SRA, Prins W, Assink D, van de Beld L, van Swaaij WPM. Gasification of biomass in supercritical water: results of micro and pilot scale experiments. In: The 2nd World Conference and Technology Exhibition on Biomass for Energy, Industry and Climate Protection. Rome 2004. p. 742–5.
- Nakamura A, Kiyonaga E, Yamamura Y, Shimizu Y, Minowa T, Noda Y, et al. Gasification of catalyst-suspended chicken manure in supercritical water. *J Chem Eng JPN* 2008;41:433–40.
- Nakamura A, Kiyonaga E, Yamamura Y, Shimizu Y, Minowa T, Noda Y, et al. Detailed analysis of heat and mass balance for supercritical water gasification. *J Chem Eng JPN* 2008;41:817–28.
- Yakaboylu O, Albrecht I, Harinck J, Smit KG, Tsalidis G-A, Di Marcello M, et al. Supercritical water gasification of biomass in fluidized bed: first results and experiences obtained from TU Delft/Gensos semi-pilot scale setup. *Biomass Bioenergy* 2018;111:330–42.
- Lu YJ, Jin H, Guo LJ, Zhang XM, Cao CQ, Guo X. Hydrogen production by biomass gasification in supercritical water with a fluidized bed reactor. *Int J Hydrogen Energy* 2008;33:6066–75.
- Lu Y, Zhao L, Guo L. Technical and economic evaluation of solar hydrogen production by supercritical water gasification of biomass in China. *Int J Hydrogen Energy* 2011;36:14349–59.
- Chen J, Lu Y, Guo L, Zhang X, Xiao P. Hydrogen production by biomass gasification in supercritical water using concentrated solar energy: system development and proof of concept. *Int J Hydrogen Energy* 2010;35:7134–41.
- Guo L, Jin H. Boiling coal in water: Hydrogen production and power generation system with zero net CO<sub>2</sub> emission based on coal and supercritical water gasification. *Int J Hydrogen Energy* 2013;38:12953–67.
- Guo L, Jin H, Lu Y. Supercritical water gasification research and development in China. *J Supercrit Fluids* 2015;96:144–50.
- Dufour J, Serrano DP, Gálvez JL, González A, Soria E, Fierro JLG. Life cycle assessment of alternatives for hydrogen production from renewable and fossil sources. *Int J Hydrogen Energy* 2012;37:1173–83.
- Renó MLG, Olmo OAd, Palacio JCE, Lora EES, Venturini OJ. Sugarcane bio-refineries: case studies applied to the Brazilian sugar-alcohol industry. *Energy Convers Manage* 2014;86:981–91.
- McManus MC, Taylor CM. The changing nature of life cycle assessment. *Biomass Bioenergy* 2015;82:13–26.
- Moreno J, Dufour J. Life cycle assessment of hydrogen production from biomass gasification. Evaluation of different Spanish feedstocks. *Int J Hydrogen Energy* 2013;38:7616–22.
- Galera S, Gutiérrez Ortiz FJ. Life cycle assessment of hydrogen and power production by supercritical water reforming of glycerol. *Energy Convers Manage* 2015;96:637–45.
- Smikova M, Jančák F, Riccardi J. Life cycle analysis of processes for hydrogen production. *Int J Hydrogen Energy* 2011;36:7844–51.
- Cetinkaya E, Dincer I, Naterer GF. Life cycle assessment of various hydrogen production methods. *Int J Hydrogen Energy* 2012;37:2071–80.
- Lu YJ, Guo LJ, Zhang XM, Yan QH. Thermodynamic modeling and analysis of biomass gasification for hydrogen production in supercritical water. *Chem Eng J*. 2007;131:233–44.
- Reddy SN, Nanda S, Dalai AK, Kozinski JA. Supercritical water gasification of biomass for hydrogen production. *Int J Hydrogen Energy* 2014;39:6912–26.
- Susanti RF, Veriansyah B, Kim J-D, Kim J, Lee Y-W. Continuous supercritical water gasification of isooctane: a promising reactor design. *Int J Hydrogen Energy*

- 2010;35:1957–70.
- [52] Matsumura Y, Minowa T, Potic B, Kersten SRA, Prins W, van Swaaij WPM, et al. Biomass gasification in near- and super-critical water: status and prospects. *Biomass Bioenergy* 2005;29:269–92.
- [53] Cocero MJ, Alonso E, Torío R, Vallelado D, Fdz-Polanco F. Supercritical Water Oxidation in a Pilot Plant of Nitrogenous Compounds: 2-Propanol Mixtures in the Temperature Range 500–750 °C. *Ind Eng Chem Res.* 2000;39:3707–16.
- [54] Safari F, Norouzi O, Tavasoli A. Hydrothermal gasification of *Cladophora glomerata* macroalgae over its hydrochar as a catalyst for hydrogen-rich gas production. *Bioresour Technol* 2016;222:232–41.
- [55] Jin H, Lu Y, Liao B, Guo L, Zhang X. Hydrogen production by coal gasification in supercritical water with a fluidized bed reactor. *Int J Hydrogen Energy* 2010;35:7151–60.
- [56] Mehmeti A, Angelis-Dimakis A, Arampatzis G, McPhail S, Ulgiati S. Life cycle assessment and water footprint of hydrogen production methods: from conventional to emerging technologies. *Environments.* 2018;5:24.
- [57] Lu YJ, Guo LJ, Ji CM, Zhang XM, Hao XH, Yan QH. Hydrogen production by biomass gasification in supercritical water: a parametric study. *Int J Hydrogen Energy* 2010;35:822–31.
- [58] Salimi M, Safari F, Tavasoli A, Shakeri A. Hydrothermal gasification of different agricultural wastes in supercritical water media for hydrogen production: a comparative study. *Int J Ind Chem* 2016;7:277–85.
- [59] Duan Z, Moller N, Weare JH. A general equation of state for supercritical fluid mixture and molecular dynamics simulation of mixture PVTX properties. *Geochim Cosmochim Acta* 1996;60(7):1209–16.
- [60] Calzavara Y, Jousot-Dubien C, Boissonnet G, Sarrade S. Evaluation of biomass gasification in supercritical water process for hydrogen production. *Energy Convers Manage* 2005;46:615–31.
- [61] Ribeiro AM, Santos JC, Rodrigues AE. PSA design for stoichiometric adjustment of bio-syngas for methanol production and co-capture of carbon dioxide. *Chem Eng J.* 2010;163:355–63.
- [62] Spath PL, Mann MK. *Life Cycle Assessment of Hydrogen Production via Natural Gas Steam Reforming.* ; National Renewable Energy Lab., Golden, CO (US); 2000. p. Medium: ED; Size: vp.
- [63] Kuenlin A, Augsburg G, Gerber L, Maréchal F. Life cycle assessment and environmental optimization of concentrating solar thermal power plants. 26th International Conference on Efficiency, Cost, Optimization, Simulation and Environmental Impact of Energy Systems (ECOS2013)2013.
- [64] ISO I. 14040: Environmental management—life cycle assessment—principles and framework. London: British Standards Institution. 2006.
- [65] Guinée JB. Handbook on life cycle assessment operational guide to the ISO standards. *Int J Life Cycle Assessment* 2002;7:311.
- [66] Ali B, Kumar A. Development of life cycle water footprints for gas-fired power generation technologies. *Energy Convers Manage* 2016;110:386–96.
- [67] Hoekstra AY. A critique on the water-scarcity weighted water footprint in LCA. *Ecol Ind* 2016;66:564–73.
- [68] Puig R, Fullana-i-Palmer P, Baquero G, Riba J-R, Bala A. A cumulative energy demand indicator (CED), life cycle based, for industrial waste management decision making. *Waste Manage* 2013;33:2789–97.
- [69] Zhao D, Han N. Optimizing overall energy harvesting performances of miniature Savonius-like wind harvesters. *Energy Convers Manage* 2018;178:311–21.
- [70] Safari F, Tavasoli A, Ataei A. Gasification of sugarcane bagasse in supercritical water media for combined hydrogen and power production: a novel approach. *Int J Environ Sci Technol* 2016;13:2393–400.
- [71] Yakaboylu O, Harinck J, Gerton Smit KG, de Jong W. Supercritical water gasification of manure: a thermodynamic equilibrium modeling approach. *Biomass Bioenergy* 2013;59:253–63.
- [72] Koroneos C, Dompros A, Roumbas G. Hydrogen production via biomass gasification—A life cycle assessment approach. *Chem Eng Process Process Intensif* 2008;47:1261–8.
- [73] Verma A, Kumar A. Life cycle assessment of hydrogen production from underground coal gasification. *Appl Energy* 2015;147:556–68.
- [74] Utgikar V, Thiesen T. Life cycle assessment of high temperature electrolysis for hydrogen production via nuclear energy. *Int J Hydrogen Energy* 2006;31:939–44.
- [75] Boese FK. Plant for thermochemical water dissociation by solar energy. US Patent 1983;4(391):793.
- [76] Naterer G, Suppiah S, Lewis M, Gabriel K, Dincer I, Rosen MA, et al. Recent Canadian advances in nuclear-based hydrogen production and the thermochemical Cu–Cl cycle. *Int J Hydrogen Energy* 2009;34:2901–17.
- [77] Ozbilen A, Dincer I, Rosen MA. Life cycle assessment of hydrogen production via thermochemical water splitting using multi-step Cu–Cl cycles. *J Cleaner Prod* 2012;33:202–16.
- [78] Lattin WC, Utgikar VP. Global warming potential of the sulfur–iodine process using life cycle assessment methodology. *Int J Hydrogen Energy* 2009;34:737–44.
- [79] Ozbilen A, Dincer I, Rosen MA. A comparative life cycle analysis of hydrogen production via thermochemical water splitting using a Cu–Cl cycle. *Int J Hydrogen Energy* 2011;36:11321–7.
- [80] Markevich M, Sonnemann GW, Castells F, Montane D. Life cycle inventory analysis of hydrogen production by the steam-reforming process: comparison between vegetable oils and fossil fuels as feedstock. *Green Chem* 2002;4:414–23.
- [81] Utgikar V, Ward B. Life cycle assessment of ISPR Mark 9 thermochemical cycle for nuclear hydrogen production. *J Chem Technol Biotechnol* 2006;81:1753–9.
- [82] Dufour J, Serrano DP, Galvez JL, Moreno J, Garcia C. Life cycle assessment of processes for hydrogen production. Environmental feasibility and reduction of greenhouse gases emissions. *Int J Hydrogen Energy* 2009;34:1370–6.